



## Chemical characterization and neuroprotective properties of copper nanoparticles green-synthesized by *nigella sativa* L. seed aqueous extract against methadone-induced cell death in adrenal pheochromocytoma (PC12) cell line

Wen Yan, Yutang Liu, Shirin Mansooridara, Atoosa Shahriyari Kalantari, Nastaran Sadeghian, Parham Taslimi, Akram Zangeneh & Mohammad Mahdi Zangeneh

To cite this article: Wen Yan, Yutang Liu, Shirin Mansooridara, Atoosa Shahriyari Kalantari, Nastaran Sadeghian, Parham Taslimi, Akram Zangeneh & Mohammad Mahdi Zangeneh (2020) Chemical characterization and neuroprotective properties of copper nanoparticles green-synthesized by *nigella sativa* L. seed aqueous extract against methadone-induced cell death in adrenal pheochromocytoma (PC12) cell line, Journal of Experimental Nanoscience, 15:1, 280-296, DOI: [10.1080/17458080.2020.1778167](https://doi.org/10.1080/17458080.2020.1778167)

To link to this article: <https://doi.org/10.1080/17458080.2020.1778167>



© 2020 The Author(s). Published by Informa UK Limited, trading as Taylor & Francis Group.



Published online: 26 Jun 2020.



[Submit your article to this journal](#)



Article views: 1506



[View related articles](#)



[View Crossmark data](#)



Citing articles: 5 [View citing articles](#)



## Chemical characterization and neuroprotective properties of copper nanoparticles green-synthesized by *nigella sativa* L. seed aqueous extract against methadone-induced cell death in adrenal pheochromocytoma (PC12) cell line

Wen Yan<sup>a</sup>, Yutang Liu<sup>b</sup>, Shirin Mansooridara<sup>c</sup>, Atoosa Shahriyari Kalantari<sup>d</sup>, Nastaran Sadeghian<sup>e</sup>, Parham Taslimi<sup>f</sup>, Akram Zangeneh<sup>g,h</sup> and Mohammad Mahdi Zangeneh<sup>g,h</sup>

<sup>a</sup>Department of Neurology, the First People's Hospital of Lanzhou, Lanzhou City, China; <sup>b</sup>Department of Neurology, Xi'an TCM Hospital of Encephalopathy, Xi'an, China; <sup>c</sup>Faculty of Medicine, Medical Sciences Research Center, Tehran Medical Sciences Branch, Islamic Azad University, Tehran, Iran; <sup>d</sup>Faculty of Medicine, Department of Neurology, Tehran Medical Sciences, Islamic Azad University, Tehran, Iran; <sup>e</sup>Faculty of Sciences, Department of Chemistry, Ataturk University, Erzurum, Turkey; <sup>f</sup>Faculty of Science, Department of Biotechnology, Bartin University, Bartin, Turkey; <sup>g</sup>Faculty of Veterinary Medicine, Department of Clinical Sciences, Razi University, Kermanshah, Iran; <sup>h</sup>Biotechnology and Medicinal Plants Research Center, Ilam University of Medical Sciences, Ilam, Iran

### ABSTRACT

Recently, scientists have used the metallic nanoparticles especially copper nanoparticles for formulating many new neuroprotective supplements in the field of neurology. Also, we know the role of *Nigella sativa* L. in increasing the physiological activities of the central nervous system in traditional medicine. In the present study, we decided to prepare and formulate a new neuroprotective supplement (copper nanoparticles in aqueous medium using *N. sativa* seed aqueous extract) in the *in vitro* condition. The organometallic chemistry tests such as Fourier Transformed Infrared Spectroscopy (FT-IR), UV-Visible Spectroscopy (UV-Vis), Field Emission Scanning Electron Microscopy (FE-SEM), and Transmission Electron Microscopy (TEM) were used for characterizing of copper nanoparticles. In the FT-IR test, the presence of many antioxidant compounds with related bonds caused excellent condition for reducing copper in the copper nanoparticles. In UV-Vis, the clear peak in the wavelength of 569 nm showed the copper nanoparticles formation. Also, in the TEM and FE-SEM images, the copper nanoparticles had the size of 19.5 nm. In the biological part of the current study, methadone significantly ( $p \leq 0.01$ ) decreased cell viability, mitochondrial membrane potential, and increased inflammatory cytokines concentrations, caspase-3 activity, and DNA fragmentation. CuNPs-treated cell cutlers significantly ( $p \leq 0.01$ ) increased cell viability and mitochondrial membrane potential, and decreased inflammatory cytokines concentrations, caspase-3 activity, and DNA

### ARTICLE HISTORY

Received 8 May 2020  
Accepted 31 May 2020

### KEYWORDS

Chemical characterization; copper nanoparticles; neuroprotective supplement; methadone; PC12

\*CONTACT Yutang Liu  [liuyutang\\_666@sina.com](mailto:liuyutang_666@sina.com)  Department of Neurology, Xi'an TCM Hospital of Encephalopathy, Xi'an, China.

© 2020 The Author(s). Published by Informa UK Limited, trading as Taylor & Francis Group.

This is an Open Access article distributed under the terms of the Creative Commons Attribution License (<http://creativecommons.org/licenses/by/4.0/>), which permits unrestricted use, distribution, and reproduction in any medium, provided the original work is properly cited.

fragmentation in the high concentration of methadone-treated adrenal pheochromocytoma (PC12) cells. For investigating the antioxidant properties of copper nanoparticles, the 2,2-diphenyl-1-picrylhydrazyl (DPPH) test was used in the presence of butylated hydroxytoluene as the positive control. The copper nanoparticles inhibited half of the DPPH molecules in the concentration of 171  $\mu\text{g/mL}$ . In this study, we concluded that copper nanoparticles biosynthesized by *N. sativa* L. seed suppressed methadone-induced cell death in PC12 cells.

## 1. Introduction

Methadone is an opioid pain medication used to treat moderate to moderately severe pain. It is a synthetic opioid that suppresses the pain signaling through the opioid and the non-opioid receptor pathways in humans and animals [1, 2]. The affinity of methadone for opioid receptors is lower than other opioids, such as morphine and heroin, and there is no specificity in binding this substance to  $\mu$ ,  $\kappa$ , and  $\delta$  opioid receptors [1–3]. Methadone abuse leads to destructive effects on different cells of the body, especially neurons [4, 5]. Degeneration of red neurons was observed in the brain of rats exposed to chronic use of this substance. These observations indicate that the cerebra does not act properly in the central nervous system of abuser rats [6]. It adversely affects the central nervous system, cardiovascular, and gastrointestinal systems [6–8]. Therefore, the importance of alternative pathways increases in analgesic effects of methadone compared to the opioid pathway [9]. The metabolism of methadone occurs in the liver and inactive metabolites are excreted through the kidneys. Therefore, in the case of high dose and chronic use, these organs suffer from toxic effects caused by methadone [8–10]. Reducing opioid effects and low addiction potential has charmed the use of this drug compared with the other opioid analgesics [9, 10]. Among the effects of methadone abuse, fatal intoxications and respiratory depression can be mentioned as well as the development of lesions in the brain [6, 7]. These effects may lead to neurotoxicity and dysfunction in central nervous cells. So, studying the effects of this substance on the nervous system seems to be necessary in order to reduce its adverse effects [5]. Previous studies have shown that lipid peroxidation plays a major role in the production of methadone-dependent cytotoxicity, as it has been observed in the chronic consumption of heroin and cocaine. It induces apoptosis through increasing the oxidative stress [6, 7]. Also, similar studies revealed that many mechanisms such as inadequate neurogenesis, apoptotic processes, mitochondrial dysfunction, and oxidative stress are important in neurotoxicity of methadone [5, 6]. One group of materials that can remove the neurotoxicity activities of the psychedelic drugs is the metallic nanoparticles [11].

Metallic nanoparticles are generally used in functions that require direct contact with the human body. In earlier times, metallic nanomaterials was used as a therapeutic material [12–15]. Among all nanoparticles, copper nanoparticles made fastidious attention because of its wide applications in optical, electrical, chemical, bioremediation, sensor, and biological field. Copper nanoparticles have a great interest because of low cost, availability and its known therapeutic activities [11]. Recently, the copper nanoparticles have been used for the treatment of a large number of disorders such as parasitic, viral, bacterial, fungal and diseases. Also, the copper nanoparticles have excellent potentials in the treatment of neurotoxicity [11]. Recently, it has been cleared that copper nanoparticles have excellent neuroprotective potentials and can raise the physiological function of the

central nervous system [11]. In a study, the positive effects of copper nanoparticles on rat cerebral microvessel endothelial cells were investigated. In the previous research, the exposure of copper nanoparticles at 1.56-50 $\mu$ g/mL concentrations raises cellular proliferation of rat brain microvessel endothelial cells. Prostaglandin E2 release was raised significantly (threefold; 8 h) for copper nanoparticles (40 and 60 nm). The extracellular levels of both TNF- $\alpha$  and IL-1b unchanged following exposure to copper nanoparticles. The P-apparent ratio, as an indicator of enhanced permeability of rat brain microvessel endothelial cells was approximately twofold for copper nanoparticles. Also, it has been shown that CuNPs can remove neurotoxin agents in the central nervous system [11].

Recently, scientists have used the neuroprotective potentials of medicinal plants for synthesizing the metallic nanoparticles containing natural compounds. So far, the neuroprotective effects of *Salvia Officinalis*, *Hypericum perforatum*, *Lavandula angustifolia*, *Opuntia ficus-indica*, *Curculigo orchioides*, *Ficus religiosa*, *Angelica sinensis*, *Cassia fistula*, *Dichrostachys cinerea*, *Panax ginseng*, *Aerva lanata*, *Juglans regai*, *Crocus sativus*, *Pongamia pinnata*, *Polygala paniculata*, *Cipura paludosa*, *Carum carvi* L., *Cymbopogon winteri-anus*, *Mentha spicata* L., *Cassia siamea*, *Galanthus nivalis* L., *Thymus vulgaris* L., and *Curcuma longa* have been proved [16]. *Nigella sativa* as a neuroprotective supplement is used in traditional medicine for the treatment of nervous disorders. *N. sativa* is from *Ranunculales* order, *Ranunculaceae* family, and *Nigella* genus. Among all parts of this species, its seed is precious in medicine. Among various medicinal plants, *N. sativa* is emerging as a miracle herb with a rich historical and religious background since many researches revealed its wide spectrum of pharmacological potential. *N. sativa* is commonly known as black seed. *N. sativa* is native to Southern Europe, North Africa and Southwest Asia and it is cultivated in many countries in the world like Middle Eastern Mediterranean region, South Europe, Iran, India, Pakistan, Syria, Turkey, Saudi Arabia [17]. The seeds of *N. sativa* and their oil have been widely used for centuries in the treatment of various ailments throughout the world. And it is an important drug in the Indian traditional system of medicine like Unani and Ayurveda. Among Muslims, it is considered as one of the greatest forms of healing medicine available due to it was mentioned that black seed is the remedy for all diseases except death in one of the Prophetic hadith. It is also recommended for use on regular basis in Tibb-e-Nabwi (Prophetic Medicine) [17]. The most antioxidant compounds of seed are thymoquinone, p-cymene, dithymoquinone, 4-terpineol,  $\alpha$ -pinene, t-anethol, thymohydroquinone, carvacrol, sesquiterpene longifolene, and thymol. The seed of *N. sativa* is used in the medicine for its antioxidant, anti-inflammatory, contraceptive, anti-fertility, testicular-protective, anticonvulsant, pulmonary-protective, anti-asthmatic, antibacterial, antifungal, antiviral, anti-parasitic, anti-schistosomiasis, gastro-protective, entero-protective, hepato-protective, nephron-protective, spleno-protective, anti-diabetic, anticancer, analgesic, immunomodulatory, especially anti-oxytocic, and neuro-pharmacological effects [17].

According to the neuroprotective properties of copper metal and *N. sativa* seed separately, we decided to prepare and formulate a new neuroprotective supplement (copper nanoparticles in aqueous medium using *N. sativa* seed aqueous extract) in the *in vitro* condition.

## 2. Experimental

### 2.1. Material

Antimycotic antibiotic solution, decamplmaneh fetal bovine serum, Dulbecco's Modified Eagle Medium (DMED), carbazole reagent, 2,2-diphenyl-1-picrylhydrazyl (DPPH), 4-(Dimethylamino)benzaldehyde, phosphate buffer solution (PBS), borax-sulphuric acid



**Figure 1.** The image of *Nigella sativa* L. seed.

mixture, Ehrlich solution, hydrolysate, and dimethyl sulfoxide (DMSO), all were achieved from Sigma-Aldrich company of USA.

## **2.2. Synthesis of CuNPs**

At the beginning of the aqueous extracting, the fresh and healthy parts of *N. sativa* (seed) were collected from Kermanshah city (Iran; [Figure 1](#)). After shade drying in a mixer, 50 g of powdered plant sample was extracted with distilled water with increase of polarity at a ratio of 1:15 (v/v). At the end, for concentrating, rotary evaporator was used [[14](#), [15](#)].

The green synthesis of the CuNPs was initiated with a reaction mixture of 20 mL of  $\text{Cu}(\text{NO}_3)_2 \cdot 3\text{H}_2\text{O}$  in the concentration of 0.05 M and 200 mL of aqueous extract solution of *N. sativa* seed (20  $\mu\text{g}/\text{mL}$ ) in the proportion 1:10 in a conical flask ([Figure 1](#)). The reaction mixture was kept under magnetic stirring for 12 h at room temperature. At the end of the reaction time, the dark green colored colloidal solution of Cu was formed. The mixture was centrifuged at 10,000 rpm for 15 min. The precipitate was triplet washed with water and centrifuged subsequently [[14](#), [15](#)].

## **2.3. Chemical characterization of CuNPs**

In this research, to record the UV-Vis spectra, a Shimadzu UV spectrophotometer was used. To investigate the size and morphology of CuNPs, Philips EM208S was employed to record transmission electron microscopy (TEM) images. Also, JASCO (FT/IR-6200) spectrophotometer was utilized to record the FT-IR spectra in this research. To evaluate the different morphological characteristic of CuNPs such as size distribution, surface

morphology and the particle shape, MIRA3TESCAN-XMU FESEM was used to record Field Emission Scanning Electron Microscopy (FESEM) images.

#### **2.4. Determination of the antioxidant property of CuNPs by DPPH**

At the beginning of the study, 100 mL of methanol (50%) was added to the 39.4 g of DPPH. Also, several concentrations of  $\text{Cu}(\text{NO}_3)_2$ , *N. sativa* seed aqueous extract, and CuNPs i.e. 0-1000  $\mu\text{g}/\text{mL}$  were considered. The above DPPH was added to the various concentrations of  $\text{Cu}(\text{NO}_3)_2$ , *N. sativa* seed aqueous extract, and CuNPs and all samples were transfer to an incubator at the temperature of  $37^\circ\text{C}$ . After 30 min incubating, the absorbances were measured at 517 nm. In this study, methanol (50%) and butylated hydroxytoluene (BHT) were negative and positive controls, respectively. According to the following formula, the antioxidant properties of  $\text{Cu}(\text{NO}_3)_2$ , *N. sativa* seed aqueous extract, and CuNPs were determined [18]:

$$\text{DPPH free radical scavenging (\%)} = (\text{Control} - \text{Test}/\text{Control}) \times 100$$

#### **2.5. Neuroprotective analyses of CuNPs**

##### **2.5.1. Cell culture**

In this experiment, adrenal pheochromocytoma (PC12; ATCC® CRL-1721<sup>TM</sup>) cells were cultured in Gibco RPMI1640 cell culture medium according to the protocols. 10% fetal bovine serum (FBS, Gibco), 100 IU/mL penicillin (Sigma), and 100  $\mu\text{g}/\text{mL}$  streptomycin (Sigma) were supplemented in cell cultures in T-25cm<sup>2</sup> tissue culture flasks and standard condition (were incubated at  $37^\circ\text{C}$  in 5%  $\text{CO}_2$ ). Methadone changes the morphology of the cells, so apoptotic cells result in the treatment of the cell by 100 mM of water diluted-methadone. For  $\text{Cu}(\text{NO}_3)_2$ , *N. sativa* seed aqueous extract, and CuNPs solutions in RPMI1640 water cell culture medium, at first, it was solved in DMSO and added to culture medium by final volume of 0.1%. Then, 12 h after the plating, the cells were washed by PBS ( $37^\circ\text{C}$ ) and classified into eight groups for 48 h. The eight groups are listed below:

Methadone: Cell culture contains 100  $\mu\text{M}$  methadone.

Control: Cell culture medium without methadone,  $\text{Cu}(\text{NO}_3)_2$ , *N. sativa* seed aqueous extract, and CuNPs.

T1: Cell culture contains 100  $\mu\text{M}$  methadone and 2  $\mu\text{g}$  of  $\text{Cu}(\text{NO}_3)_2$ .

T2: Cell culture contains 100  $\mu\text{M}$  methadone and 4  $\mu\text{g}$  of  $\text{Cu}(\text{NO}_3)_2$ .

T3: Cell culture contains 100  $\mu\text{M}$  methadone and 2  $\mu\text{g}$  of *N. sativa* seed aqueous extract.

T4: Cell culture contains 100  $\mu\text{M}$  methadone and 4  $\mu\text{g}$  of *N. sativa* seed aqueous extract.

T5: Cell culture contains 100  $\mu\text{M}$  methadone and 2  $\mu\text{g}$  of CuNPs.

T6: Cell culture contains 100  $\mu\text{M}$  methadone and 4  $\mu\text{g}$  of CuNPs.

##### **2.5.2. Cell viability**

Trypan blue was used for assessing the cell viability. The vital dye penetrates damaged or dead cells whose membranes are broken, and as a result, dead cells appear on blue lobes on the Neubauer Lamella. The cells were plated in 96 well cell culture plates with  $5 \times 10^4$  cells/mL densities for 12 h, then, they were cultured by several treatments of I-VII and incubated at  $37^\circ\text{C}$  in 5%  $\text{CO}_2$  for 48 h. After trypsinization of the cells, 200  $\mu\text{L}$  of cell suspension was mixed with 40  $\mu\text{L}$  of Trypan blue 0.4% and suspended after 2-3 min by the

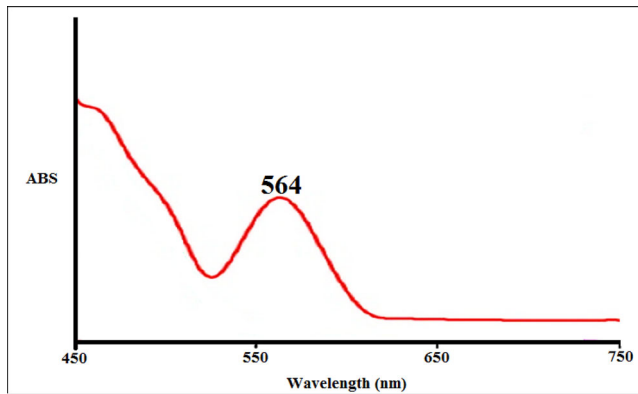


**Figure 2.** The UV-Vis spectrum of biosynthesized copper nanoparticles.

Neubauer Lamela. By following formula, the cell viability of all samples was determined [19]:

$$\text{Cell viability: } \frac{\text{Non-colored cells number}}{\text{Total cells number}}$$

### 2.5.3. Cell death index

For determining of PC12 cell death index in the different treatments of I-VII, TUNEL staining was used. Eight randomly wells were selected to counting the TUNEL positive cells by an Olympus AX-70 fluorescent microscope. The cell death index is equal to the ratio of apoptotic cells to total cells [20].

### 2.5.4. Secretion of inflammatory cytokines

The concentrations of pro-inflammatory cytokines IL-1 $\beta$ , IL-6, and TNF $\alpha$  were measured using Rat V-Plex Kit.

### 2.5.5. Mitochondrial membrane potential (MMP)

Different treatments were exposed to 10 mg/mL rhodamine-123 for a half-hour. Then, the cell was washed by PBS. In continuing, 900  $\mu$ L triton X-100 was added to each well and kept in 4 $^{\circ}$ C for 2 h. The solutions were moved to microtubes for centrifuging at 16,000 rpm for 20 min. A fluorescence microplate reader (488 nm excitation and 520 nm emission) was used for the measurement of fluorescence absorbance in the cells [21].

### 2.5.6. Caspase-3 activity

For plating PC12 cells, the well cell culture plate containing PRMI1640 medium was used. After 12 h, the plate was washed by PBS. Then, the different treatments of I-VII were added to the cells. Trypsin was used for separating the cells from the flask. For removing the supernatant, all samples were centrifuged for 10 min, then the centrifuging was done by adding lysate buffer and final they were transferred to the well cell culture plate. Later, 5  $\mu$ L N-acetyl-Asp-Glu-Val-Asp-p-nitroanilineDEVD-pNA was added to the well cell culture plate and incubated in 37 $^{\circ}$ C for 2 h. Then, releasing of pNA in a result of caspase-3 activity was recorded by Biotek (USA) Spectrophotometer [21].



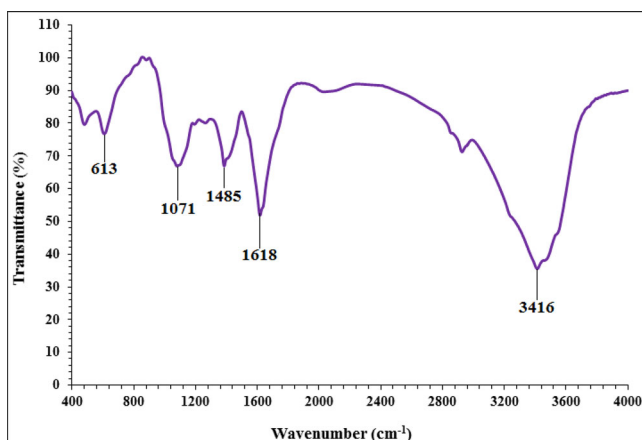


Figure 3. FT-IR spectra of biosynthesized copper nanoparticles.

## 2.6. Statistical analysis

The obtained results were fed into SPSS-22 software and analyzed by one-way ANOVA, followed by Tukeys post-hoc test ( $p \leq 0.01$ ).

## 3. Results and discussion

### 3.1. Uv-visible spectroscopy

UV-Vis spectroscopic analysis showed the presence of absorption peak at 564 nm which confirmed the formation of the copper nanoparticles (Figure 2). Rajesh *et al.* (2018) reported *Shewanella aromaticum* bud extracts synthesized CuNPs with a peak at 580 nm in the UV-Vis spectrum [22]. Zangeneh *et al.* (2019) revealed the absorbance at 572 nm for copper nanoparticles synthesized by *Falcaria vulgaris* [15]. Tahvilian *et al.* (2019) observed the peak of copper nanoparticles containing *Allium saralicum* at the wavelength of 576 nm [14]. Ramya Devi *et al.* (2012) reported the absorbance at 580 nm for copper nanoparticles through the polyol method [23]. Niharika Nagar *et al.* (2018) studied *Azadirachta indica* extracts mediated synthesis of CuNPs. Absorption in the spectrum was noted in the range between 550-600 nm [24]. Two absorbance peaks at 370 and 690 nm was shown marine endophytic actinomycetes mediated CuNPs due to two various morphological sizes of nanoparticles were synthesized [25]. Khani *et al.* (2018) reported *Ziziphus Spina-Christi* fruit extract mediated CuNPs and absorption peak was observed at 586 nm [26]. These reports support the results of the current work. The *N. sativa* seed aqueous extract mediated synthesis of CuNPs showed good stability even after 20 days and no considerable changes occurred in UV-absorbance.

### 3.2. Ft-IR analysis

In the FT-IR test, the antioxidant and secondary compounds are determined based on several peaks in special wavelengths. The analysis of the IR spectra of the copper nanoparticles revealed the peaks at 613, 1071, 1485, 1618, and 3416  $\text{cm}^{-1}$  related to the Cu-O, C-OH, C=O, C-O, and OH, respectively (Figure 3). The IR spectra investigated for the copper nanoparticles revealed the absorption peaks at (I) 3287  $\text{cm}^{-1}$  (OH group of



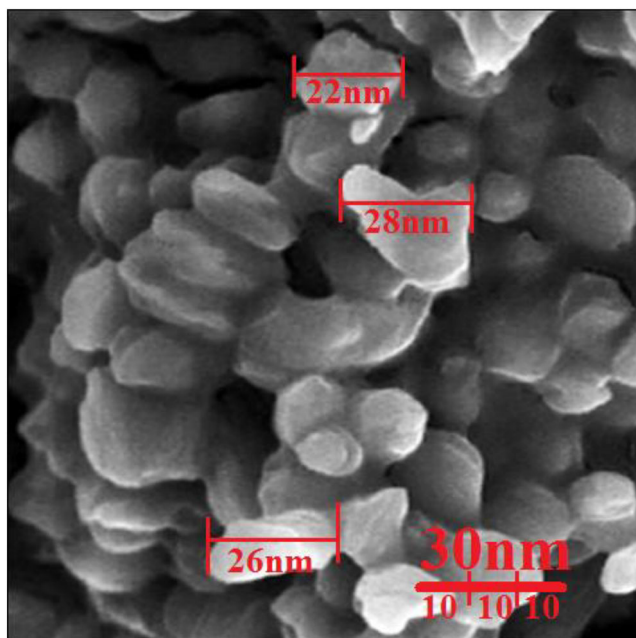


Figure 4. FE-SEM image of copper nanoparticles.

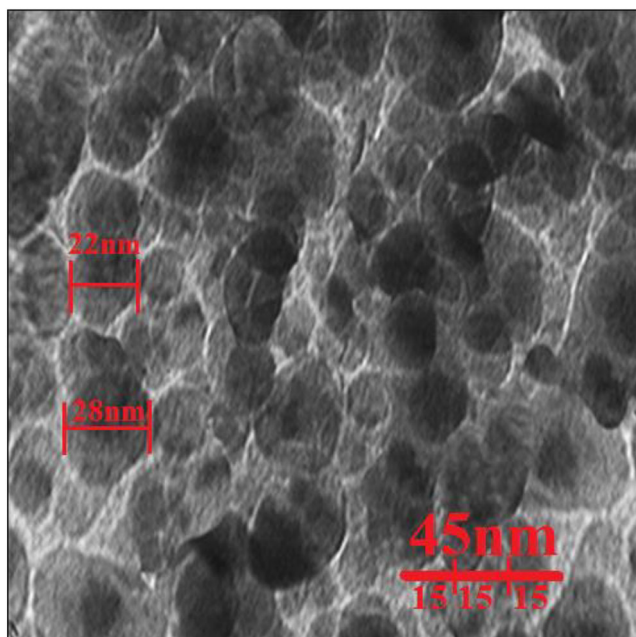
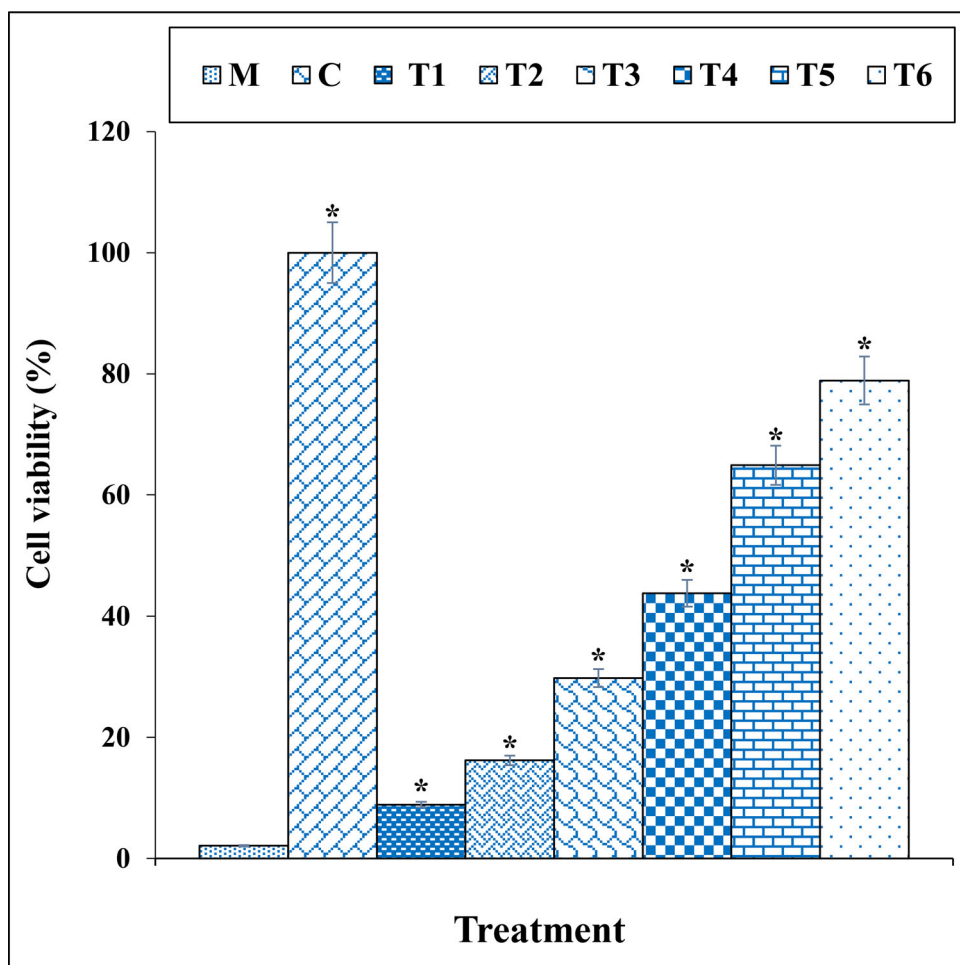


Figure 5. TEM image of copper nanoparticles.

alcohols and phenols); (II)  $1623\text{ cm}^{-1}$  (C-O group of carboxylic acid group); (III)  $1383\text{ cm}^{-1}$  (C=O stretching of carboxylic acid group); (IV)  $1038\text{ cm}^{-1}$  (C-OH vibrations of the protein/polysaccharide) [4, 15, 22–26].



**Figure 6.** The cell viability of different treatments after 48 h.

M: Methadone, C: Control, T1: 100 $\mu$ M methadone and 2 $\mu$ g of Cu(NO<sub>3</sub>)<sub>2</sub>, T2: 100 $\mu$ M methadone and 4 $\mu$ g of Cu(NO<sub>3</sub>)<sub>2</sub>, T3: 100 $\mu$ M methadone and 2 $\mu$ g of *N. sativa*, T4: 100 $\mu$ M methadone and 4 $\mu$ g of *N. sativa*, T5: 100 $\mu$ M methadone and 2 $\mu$ g of CuNPs, T6: 100 $\mu$ M methadone and 4 $\mu$ g of CuNPs.

\*indicate the significant difference ( $p < 0.01$ ) between experimental groups with methadone group.

### 3.3. Fe-SEM and TEM analysis

The FE-SEM image of copper nanoparticles is shown in Figure 4. The copper nanoparticles appeared as an agglomerated structure. The hydroxyl groups present in *N. sativa* seed aqueous extract could be responsible for agglomeration [23]. Also, FE-SEM images indicated the average size of 19.5 nm and the shape of spherical for copper nanoparticles. Many similar observations are noted by Rajesh *et al.* (2018) [22], Zangeneh *et al.* (2019) [15], Tahvilian *et al.* (2019) [14], Ramya Devi *et al.* (2012) [23], Niharika Nagar *et al.* (2018) [24], and Khani *et al.* (2018) [26].

Also, the average size of the nanoparticles (19.5 nm) calculated through TEM images (Figure 5). Furthermore, the histogram plot from the TEM image showed the particle size distribution of biosynthesized copper nanoparticles ranges of 7 to 27 nm. In the previous studies, the size of copper nanoparticles formulated by aqueous extract of medicinal plants

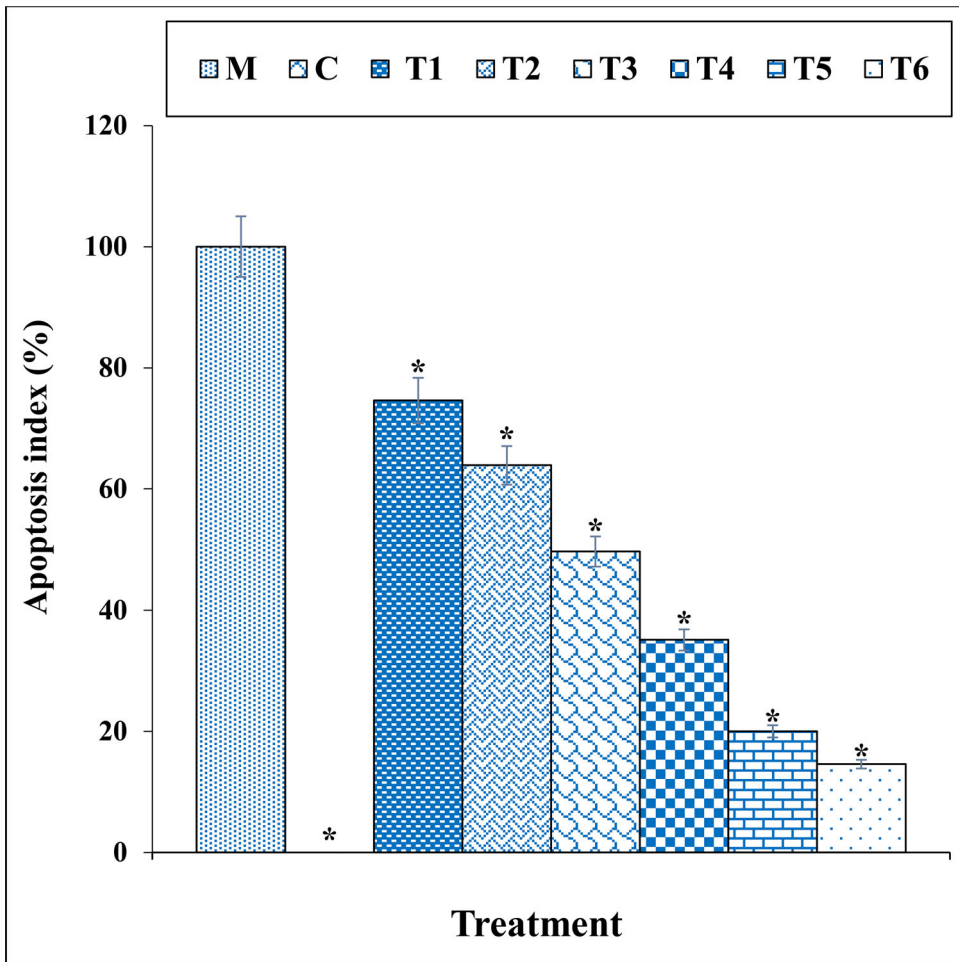


**Figure 7.** The apoptosis index of different treatments after 48 h.

M: Methadone, C: Control, T1: 100 $\mu$ M methadone and 2 $\mu$ g of Cu(NO<sub>3</sub>)<sub>2</sub>, T2: 100 $\mu$ M methadone and 4 $\mu$ g of Cu(NO<sub>3</sub>)<sub>2</sub>, T3: 100 $\mu$ M methadone and 2 $\mu$ g of *N. sativa*, T4: 100 $\mu$ M methadone and 4 $\mu$ g of *N. sativa*, T5: 100 $\mu$ M methadone and 2 $\mu$ g of CuNPs, T6: 100 $\mu$ M methadone and 4 $\mu$ g of CuNPs.

\*indicate the significant difference ( $p < 0.01$ ) between experimental groups with methadone group.

had been calculated in the ranges of 10-40 nm with the shape of spherical [4, 15, 22–26]. These reports support the results of the current work.

### 3.4. Neuroprotective activities of CuNPs

Methadone is prescribed as an analgesic and may be of concern because of its addictive potential or side effects [27, 28]. Abuse of this drug, like other opioid compounds, may affect the central nervous system cells by affecting the opioid signaling pathway also, its metabolites may be harmful to the digestive and excretion system [29, 30]. The pathway for the breakdown of methadone passes through the liver and kidneys, therefore the potential of side effects is high in these organs [6, 7] Also, methadone severely affects white matter [31, 32]. Li *et al.* (2016) indicated that methadone destroyed the white matter integrity and caused many peripheral neuropathies [33]. Two researchers revealed the

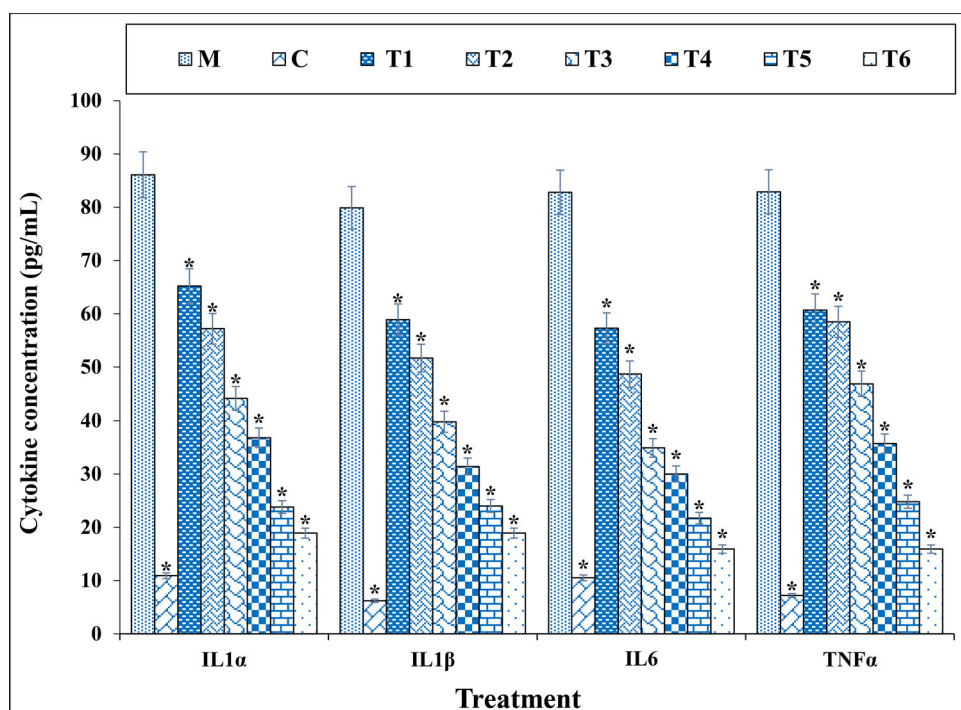


**Figure 8.** The cytokine concentration in different treatments after 48 h.

M: Methadone, C: Control, T1: 100 $\mu$ M methadone and 2 $\mu$ g of Cu(NO<sub>3</sub>)<sub>2</sub>, T2: 100 $\mu$ M methadone and 4 $\mu$ g of Cu(NO<sub>3</sub>)<sub>2</sub>, T3: 100 $\mu$ M methadone and 2 $\mu$ g of *N. sativa*, T4: 100 $\mu$ M methadone and 4 $\mu$ g of *N. sativa*, T5: 100 $\mu$ M methadone and 2 $\mu$ g of CuNPs, T6: 100 $\mu$ M methadone and 4 $\mu$ g of CuNPs.

\*indicate the significant difference ( $p \leq 0.01$ ) between experimental groups with methadone group.

effects of methadone on the lung and brain (cerebral cortex and hippocampus) of rats. They emphasized the role of oxidative stress, neuronal, and pulmonary damage in disruptive effects of methadone abuse [34, 35]. Methadone is caused the neurotoxicity by two ways; in first way, it is bound to the opioid receptors and affects the neurons, in second way, methadone destroys by antagonist acting in NMDR. The previous observations have indicated that second way is more effective than the first way in cytotoxicity of neural cells [36]. Also, methadone has direct effects on the central nervous system and increases the reactive oxygen species (ROS) by reducing the level of antioxidant activity in the plasma. Therefore, it seems necessary to evaluate the toxic effect of methadone in neuron cells and study on compounds which can decline these toxic effects [35]. Chan *et al.* (2015) indicted the immunotoxicity properties of methadone inside of the neurotoxicity effects. In the previous study, methadone increased the pro-inflammatory cytokines such as interleukin 1 [37]. The cytotoxicity properties of methadone increase significantly the cell death and reduce the cell proliferation in nerve cells [37]. Friesen *et al.* (2008) showed that methadone through apoptosis induction, caspase-3 and caspase-9 activation, and cell proliferation inhibition induced cell death in acute and chronic leukemia cells [38]. The findings of our experiment also agreed with these results and revealed that methadone at high concentrations reduced significantly ( $p \leq 0.01$ ) cell viability and increased inflammatory cytokines concentrations and caspase-3 activity. Treatment of these cells with both doses of copper nanoparticles synthesized using *N. sativa* seed aqueous extract increased the cell proliferation and cell viability potentials due to the cell cytotoxicity reduction (Figures 6–9).

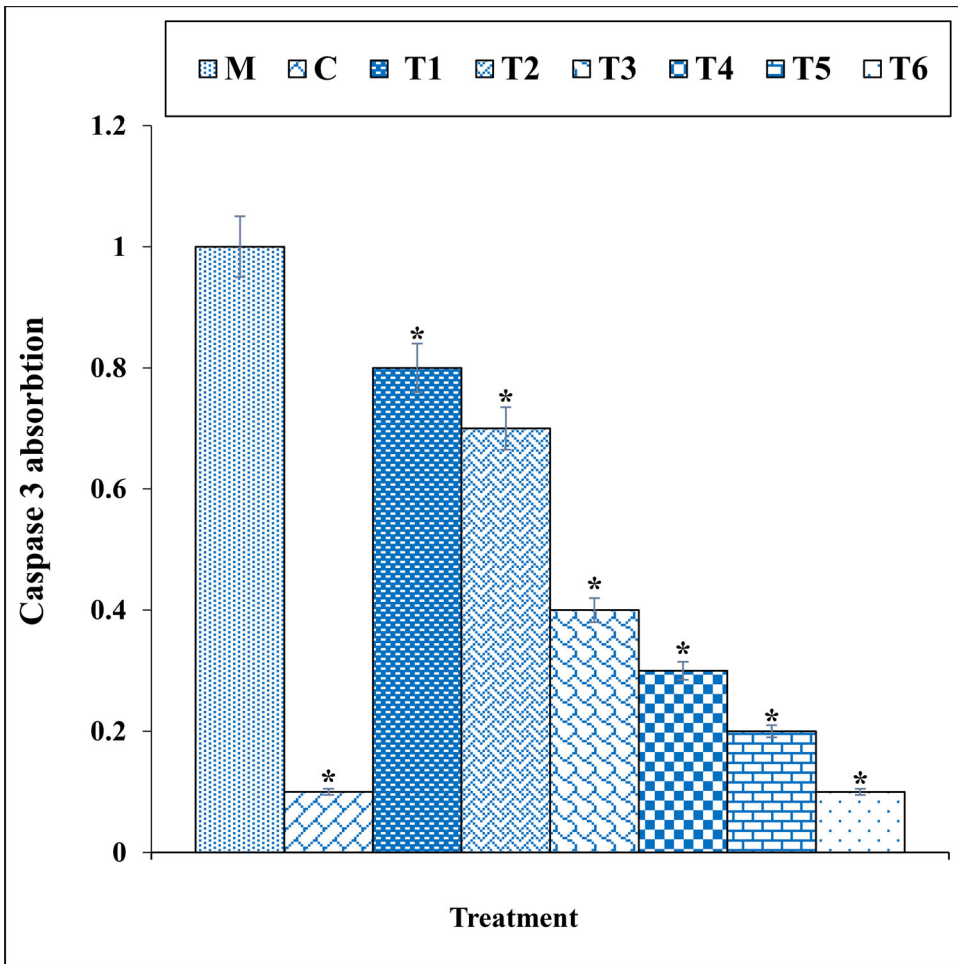


**Figure 9.** The caspase 3 absorption in different treatments after 48 h. M: Methadone, C: Control, T1: 100µM methadone and 2µg of Cu(NO<sub>3</sub>)<sub>2</sub>, T2: 100µM methadone and 4µg of Cu(NO<sub>3</sub>)<sub>2</sub>, T3: 100µM methadone and 2µg of *N. sativa*, T4: 100µM methadone and 4µg of *N. sativa*, T5: 100µM methadone and 2µg of CuNPs, T6: 100µM methadone and 4µg of CuNPs. \*indicate the significant difference ( $p \leq 0.01$ ) between experimental groups with methadone group.

The previous studies indicated that methadone produced many free radicals especially ROS in the body [39–41]. Free radicals with degradation of DNA molecules cause cellular degradation and apoptosis in the cells [39]. Also, ROS directly damages the DNA and increase the apoptosis in neurons through production of free-radicals [39, 40]. In our study, the experiment of apoptosis by the TUNEL test indicated that methadone caused DNA fragmentation and induced apoptosis in nerve-like PC12 cells. Further experiments revealed that methadone causes apoptosis in these cells by reducing the mitochondrial membrane potential. Our findings also indicated that copper nanoparticles synthesized using *N. sativa* seed aqueous extract significantly ( $p \leq 0.01$ ) increased the mitochondrial membrane potential and reduced the rate of DNA fragmentation in PC12 cells treated with methadone (Figure 10).

### 3.5. Antioxidant properties of copper nanoparticles synthesized using *N. sativa*

In our study, the antioxidant effects of the copper nanoparticles synthesized using *N. sativa* seed aqueous extract were evaluated by DPPH assay revealed concentration-dependent



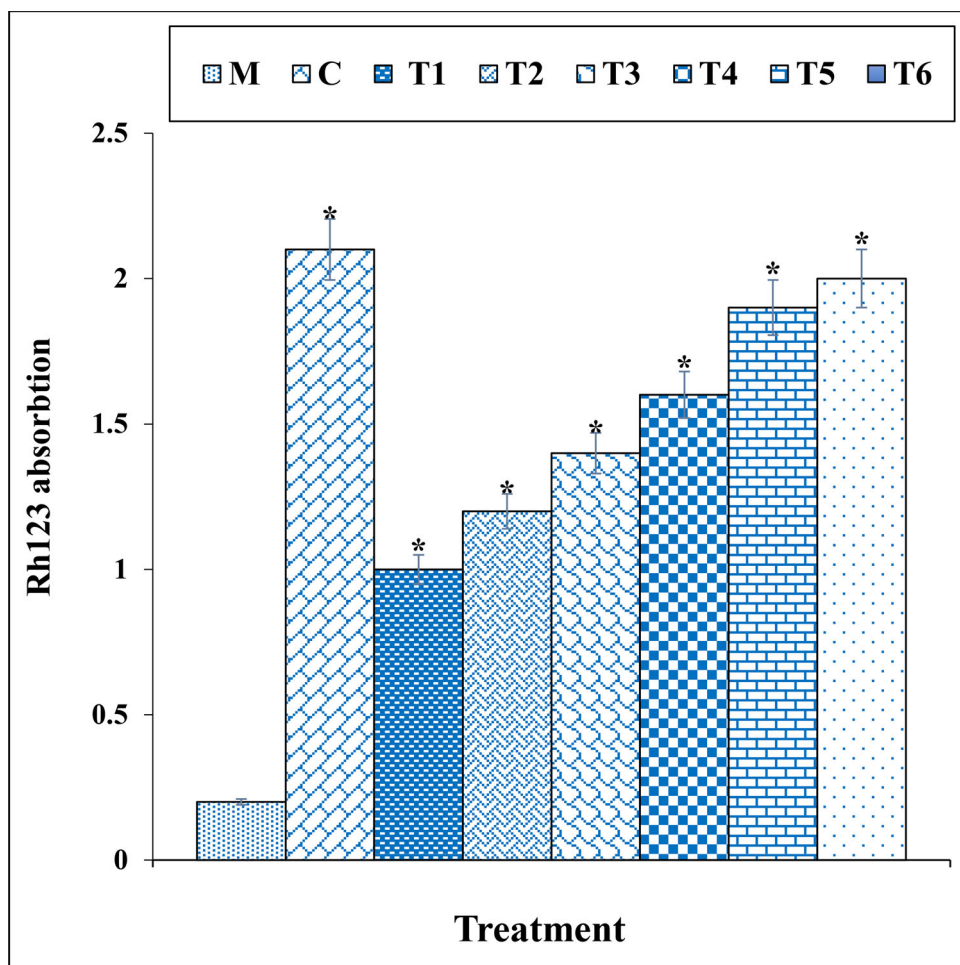


**Figure 10.** The mitochondrial membrane potential of different treatments after 48 h.

M: Methadone, C: Control, T1: 100 $\mu$ M methadone and 2 $\mu$ g of  $\text{Cu}(\text{NO}_3)_2$ , T2: 100 $\mu$ M methadone and 4 $\mu$ g of  $\text{Cu}(\text{NO}_3)_2$ , T3: 100 $\mu$ M methadone and 2 $\mu$ g of *N. sativa*, T4: 100 $\mu$ M methadone and 4 $\mu$ g of *N. sativa*, T5: 100 $\mu$ M methadone and 2 $\mu$ g of CuNPs, T6: 100 $\mu$ M methadone and 4 $\mu$ g of CuNPs.

\*indicate the significant difference ( $p < 0.01$ ) between experimental groups with methadone group.

effects i.e. an increase in the concentration of the copper nanoparticles leads to an increase in antioxidant activities. In the concentrations of studied, the best result was seen in the high concentration or 1000  $\mu$ g/mL (Figure 11).

Comparative analysis of the individual antioxidant assays showed significant variations in the exertion of radical scavenging effects. Among all materials tested ( $\text{Cu}(\text{NO}_3)_2$ , *N. sativa*, and CuNPs), the copper nanoparticles indicated more excellent inhibition effects against DPPH. In contrast, standard (butylated hydroxytoluene) demonstrated lower antioxidant effects compared to the copper nanoparticles. The IC<sub>50</sub> of *N. sativa*, butylated hydroxytoluene, and CuNPs were 308, 236, and 171  $\mu$ g/mL, respectively.

The synthesized copper nanoparticles exhibit higher antioxidant activity for the deformation of free radicals into the living system [42]. The copper nanoparticles have redox properties and play a significant role in deactivating free radicals in the living system [43]. In recent years, researchers evaluated plants and bio mediated synthesized nanoparticles for antioxidant activity. The reason behind the antioxidant activity of green or

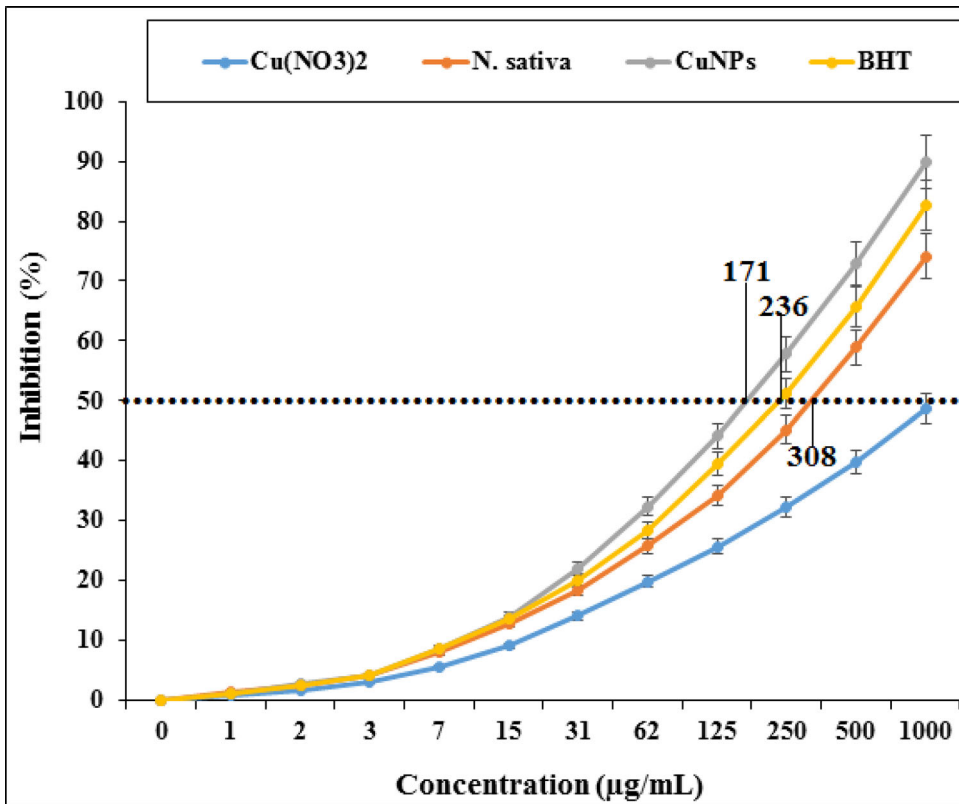


Figure 11. The antioxidant properties of Cu(NO<sub>3</sub>)<sub>2</sub>, *N. sativa*, CuNPs, and BHT against DPPH.

biosynthesized nanoparticles could be due to the presence of metabolites compounds such as phenolic compounds, flavonoids, carbohydrates, and other sugar substances [44–47]. Also, many researchers reported phenolic and flavonoids attached to the nanoparticles exhibited the antioxidant activity. Previously has been indicated that *N. sativa* is rich in antioxidant compounds such as thymol, sesquiterpene longifolene, carvacrol, thymohydroquinone,  $\alpha$ -pinene, t-anethol, dithymoquinone, 4-terpineol, p-cymene, and thymoquinone [47]. Several studies were carried out in the nanotechnology field using various medicinal plants, but still, no report is available on copper nanoparticles synthesized using *N. sativa* seed aqueous extract.

It seems that CuNPs, due to its antioxidant potential, significantly ( $p \leq 0.01$ ) increased cell viability and mitochondrial membrane potential, and decreased inflammatory cytokines concentrations, caspase-3 activity, and DNA fragmentation in the high concentration of methadone-treated PC12 cells. Today, antioxidants are introduced as a reducer of cell cytotoxicity because they inhibit the reactive oxygen species production and oxidative stresses in the cells [11].

#### 4. Conclusion

*Nigella sativa* L. seed harvested from the Kermanshah city, Iran was used for synthesizing copper nanoparticles as a suitable and safe material. After copper nanoparticles synthesizing, they were characterized and analyzed by UV-Vis. and FT-IR spectroscopy, FE-SEM,



and TEM. The above tests indicated that these nanoparticles were synthesized as the best possible form.

In the biological experiments, we concluded that a high dose of methadone causes cell death in nerve-like PC12 cells through induction of cell inflammation and apoptosis. CuNPs enhanced cell viability in a high dose of methadone-treated PC12 cells. It repressed inflammatory cytokines (IL-1 $\beta$ , IL-6, and TNF- $\alpha$ ) production, mitochondrial membrane disruption, and caspase 3 activity. These events reveal that CuNPs repressed methadone-induced cell death in PC12 cells, in a dose-dependent manner.

In the future, CuNPs can be consumed for increasing the physiological activity of the central nervous system.

## Disclosure statement

No potential conflict of interest was reported by the author(s).

## References

1. de Vos JW, Ufkes JG, *L*-methadone and *D,L*-methadone in methadone maintenance treatment: a comparison of therapeutic effectiveness and plasma concentrations. *Eur Addict Res.* 1998;4(3): 134–141. C.D, Kaplan M, Tursch JK, Krause H. van Wilgenburg
2. Quillinan N, Lau EK, Virk M, et al. Recovery from mu-opioid receptor desensitization after chronic treatment with morphine and methadone. *J Neurosci.* 2011;31(12):4434–4443.
3. Gorman AL, Elliott KJ, Inturrisi CE. The *d*- and *l*-isomers of methadone bind to the non-competitive site on the N-methyl-D-aspartate (NMDA) receptor in rat forebrain and spinal cord. *Neurosci Lett.* 1997;223(1):5–8.
4. Leppert W. The role of methadone in cancer pain treatment—a review. *Int J Clin Pract.* 2009;63(7): 1095–1109.
5. Perez-Alvarez S, Cuenca-Lopez MD, De Mera RMMF, et al. Methadone induces necrotic-like cell death in SH-SY5Y cells by an impairment of mitochondrial ATP synthesis. *Biochim Biophys Acta.* 2010;1802(11):1036–1047.
6. Reig F, Busquets M, Haro I, et al. Interaction of opiate molecules with lipid monolayers and liposomes. *J Pharm Sci.* 1992;81(6):546–550.
7. McLaughlin PJ, Levin RJ, Zagon IS. *Inter. J. Oncol.* 1999;14:991–999.
8. Mintzer MZ, Stitzer ML. Cognitive impairment in methadone maintenance patients. *Drug Alcohol Depen.* 2002;67(1):41–51.
9. Rass O, Kleykamp BA, Vandrey RG, et al. Cognitive performance in methadone maintenance patients: effects of time relative to dosing and maintenance dose level. *Exp Clin Psychopharmacol.* 2014;22(3):248–256.
10. Vergun O, Sobolevsky AI, Yelshansky MV, et al. Exploration of the role of reactive oxygen species in glutamate neurotoxicity in rat hippocampal neurones in culture. *J Physiol (Lond).* 2001;531(Pt 1):147–163.
11. Trickler WJ, Lantz SM, Schrand AM, et al. Effects of copper nanoparticles on rat cerebral microvessel endothelial cells. *Nanomedicine.* 2012;7(6):835–846.
12. (a) Hemmati S, Joshani Z, Zangeneh A, Zangeneh MM. *Appl Organometal Chem.* 2019;33:e5277. (b) Hemmati S, Irani P, Zangeneh A, Zangeneh MM. *Appl Organometal Chem.* 2019;33:e5274. DOI:10.1002/aoc.5274. (c) Zangeneh MM, *Appl Organometal Chem.* 2019;33:e5295. DOI:10.1002/aoc.5295. (d) Mohammadi G, Zangeneh MM, Zangeneh A, Siavosh Haghighi ZM. *Appl Organometal Chem.* 2019;33:e5136. DOI:10.1002/aoc.5136. (e) Zangeneh MM, Bovandi S, Gharehyakheh S, Zangeneh A, Irani P. *Appl Organometal Chem.* 2019;33:e4961. (f) Hamelian M, Zangeneh MM, Shahmohammadi A, Varmira K, Veisi H. *Appl Organometal Chem.* 2019;33:e5278. DOI:10.1002/aoc.5278. (g) Hemmati S, Rashtiani A, Zangeneh MM, Mohammadi P, Zangeneh A, Veisi H. *Polyhedron.* 2019;158:8–14. (h) Zangeneh MM, Joshani Z, Zangeneh A, Miri E. *Appl Organometal Chem.* 2019;33:e5016. (i) Zangeneh A, Zangeneh MM, Moradi R. *Appl Organometal Chem.* 2019;33:e5247. DOI: 10.1002/aoc.5247.

13. (a) Zangeneh MM, Zangeneh A, Pirabbasi E, Moradi R, Almasi M. *Appl Organometal Chem.* 2019; 33:e5246. (b) Mahdavi B, Paydarfard S, Zangeneh MM, Goorani S, Seydi N, Zangeneh A. *Appl Organometal Chem.* 2019;33:e5248. DOI:10.1002/aoc.5248. (c) Jalalvand AR, Zhaleh M, Goorani S, Zangeneh MM, Seydi N, Zangeneh A, Moradi R. *Photochem J. Photobiol. B.* 2019;192:103–112. (d) Zangeneh A, Zangeneh MM. *Appl Organometal Chem.* 2019;33:e5290. DOI:10.1002/aoc.5290. (e) Hemmati S, Joshani Z, Zangeneh A, Zangeneh MM. *Appl Organometal Chem.* 2019;33:e5267. DOI: 10.1002/aoc.5267. (f) Zhaleh M, Zangeneh A, Goorani S, Seydi N, Zangeneh MM, Tahvilian R, Pirabbasi E. *Appl Organometal Chem.* 2019;33:e5015. (g) Shahriari M, Hemmati S, Zangeneh A, Zangeneh MM. *Appl Organometal Chem.* 2019;33:e5189. DOI: 10.1002/aoc.5189. (h) Zangeneh MM, Saneei S, Zangeneh A, Touthmalani R, Haddadi A, Almasi M, Amiri-Paryan A. *Appl Organometal Chem.* 2019;33:e5216. DOI: 10.1002/aoc.5216.
14. Tahvilian R, Zangeneh MM, Falahi H, et al. Green synthesis and chemical characterization of copper nanoparticles using *Allium saralicum* leaves and assessment of their cytotoxicity, antioxidant, antimicrobial, and cutaneous wound healing properties. *Appl Organomet Chem.* 2019;33:e5234.
15. Zangeneh MM, Ghaneialvar H, Akbaribazm M, et al. Novel synthesis of *Falcaria vulgaris* leaf extract conjugated copper nanoparticles with potent cytotoxicity, antioxidant, antifungal, antibacterial, and cutaneous wound healing activities under in vitro and in vivo condition. *J Photochem Photobiol B, Biol.* 2019;197:111556.
16. Mohebbati R, Khazdair MR, Hedayati M. *J. Rep. Pharma. Sci.* 2017;6:34–50.
17. Ahmad A, Husain A, Mujeeb M, et al. A review on therapeutic potential of *Nigella sativa*: A miracle herb. *Asian Pac J Trop Biomed.* 2013;3(5):337–352.
18. Hosseinimehr SJ, Mahmoudzadeh A, Ahmadi A, et al. The radioprotective effect of *Zataria multiflora* against genotoxicity induced by  $\gamma$  irradiation in human blood lymphocytes. *Cancer Biother Radiopharm.* 2011;26(3):325–329.
19. Strober W. *Curr. Protoc. Immunol.* 2015;111:1–3.
20. Byrne A, Southgate J, Brison D, et al. Analysis of apoptosis in the preimplantation bovine embryo using TUNEL. *J. Reprod. Infertil.* 1999;117(1):97–105.
21. Baracca A, Sgarbi G, Solaini G, et al. Rhodamine 123 as a probe of mitochondrial membrane potential: evaluation of proton flux through F<sub>0</sub> during ATP synthesis. *Biochim. Biophys. Acta. Bioenerg.* 2003;1606(1-3):137–146.
22. Rajesh KM, Ajitha B, Reddy YA, et al. Assisted green synthesis of copper nanoparticles using *Syzygium aromaticum* bud extract: Physical, optical and antimicrobial properties. *Optik.* 2018;154: 593–600.
23. Ramyadevi J, Jeyasubramanian K, Marikani A, et al. Synthesis and antimicrobial activity of copper nanoparticles. *Mater. Lett.* 2012;71:114–146.
24. Nagar N, Devra V. Green synthesis and characterization of copper nanoparticles using *Azadirachta indica* leaves. *Mat. Chem. Phy.* 2018;213:44–51.
25. Rasool U, Hemalatha S. Marine endophytic actinomycetes assisted synthesis of copper nanoparticles (CuNPs): Characterization and antibacterial efficacy against human pathogens. *Mater. Lett.* 2017; 194:176–180.
26. Khani R, Roostaei B, Bagherzade G, et al. Green synthesis of copper nanoparticles by fruit extract of *Ziziphus spina-christi* (L.) Willd.: application for adsorption of triphenylmethane dye and antibacterial assay. *J. Mol. Liq.* 2018;255:541–549.
27. Alford DP, Compton P, Samet JH. Acute pain management for patients receiving maintenance methadone or buprenorphine therapy. *Ann Intern Med.* 2006;144(2):127–134.
28. Beheshtkhoo N, Kouhbanani MAJ, Savardashtaki A, et al. Green synthesis of iron oxide nanoparticles by aqueous leaf extract of *Daphne mezereum* as a novel dye removing material. *Appl Phys A.* 2018;124(5):363–369.
29. Smith HS. Opioid metabolism. *Mayo Clin Proc.* 2009;84(7):613–624. editor Elsevier.
30. Atici S, Cinel I, Cinel L, et al. Liver and kidney toxicity in chronic use of opioids: An experimental long term treatment model. *J Biosci.* 2005;30(2):245–252.
31. Inturrisi C. Pharmacology of methadone and its isomers. *Minerva Anesthesiol.* 2005;71(7-8):435–437.
32. Zanin A, Masiero S, Severino MS, et al. A delayed methadone encephalopathy: clinical and neuro-radiological findings. *J Child Neurol.* 2010;25(6):748–751.
33. Li W, Li Q, Wang Y, et al. Methadone-induced damage to white matter integrity in methadone maintenance patients: a longitudinal self-control DTI study. *Sci Rep.* 2016;6:19662
34. Cerase A, Leonini S, Bellini M, et al. Methadone-induced toxic leukoencephalopathy: diagnosis and follow-up by magnetic resonance imaging including diffusion-weighted imaging and apparent diffusion coefficient maps. *J Neuroimaging.* 2011;21(3):283–286.

35. Corré J, Pillot J, Hilbert G. Methadone-induced toxic brain damage. *Case. Rep. Radiol.* 2013;2013:1–2.
36. Sotgiu ML, Valente M, Storchi R, et al. Cooperative N-methyl-D-aspartate (NMDA) receptor antagonism and mu-opioid receptor agonism mediate the methadone inhibition of the spinal neuron pain-related hyperactivity in a rat model of neuropathic pain. *Pharmacol Res.* 2009;60(4):284–290.
37. Chan YY, Yang SN, Lin JC, et al. Inflammatory response in heroin addicts undergoing methadone maintenance treatment. *Psychiatry Res.* 2015;226(1):230–234.
38. Friesen C, Roscher M, Alt A, et al. Methadone, commonly used as maintenance medication for out-patient treatment of opioid dependence, kills leukemia cells and overcomes chemoresistance. *Cancer Res.* 2008;68(15):6059–6064.
39. Kroemer G. The proto-oncogene Bcl-2 and its role in regulating apoptosis. *Nat Med.* 1997;3(6):614–620.
40. Kaufmann SH, Earnshaw WC. Induction of apoptosis by cancer chemotherapy. *Exp Cell Res.* 2000;256(1):42–49.
41. Hengartner MO. The biochemistry of apoptosis. *Nature.* 2000;407(6805):770–776.
42. Reuter S, Gupta SC, Chaturvedi MM, et al. Oxidative stress, inflammation, and cancer: How are they linked? *Free Radic Biol Med.* 2010;49(11):1603–1616.
43. Gultekin DD, Gungor AA, Onem H, et al. Synthesis of copper nanoparticles using a different method: determination of its antioxidant and antimicrobial activity. *Chem. Soc A: Chem.* 2016;3(3):623–636.
44. Rehana D, Mahendiran D, Kumar RS, et al. Evaluation of antioxidant and anticancer activity of copper oxide nanoparticles synthesized using medicinally important plant extracts. *Biomed Pharmacother.* 2017;89:1067–1077.
45. Del Mar Delgado-Povedano M, De Medina VS, Bautista J, et al. Tentative identification of the composition of *Agaricus bisporus* aqueous enzymatic extracts with antiviral activity against HCV: A study by liquid chromatography–tandem mass spectrometry in high resolution mode. *J Function. Foods.* 2016;24:403–419.
46. Jeong SC, Koyyalamudi SR, Jeong YT, et al. Macrophage immunomodulating and antitumor activities of polysaccharides isolated from *agaricus bisporus* white button mushrooms. *J Med Food.* 2012;15(1):58–65.
47. Sankar R, Maheswari R, Karthik S, et al. Anticancer activity of *Ficus religiosa* engineered copper oxide nanoparticles. *Mater Sci Eng C Mater Biol Appl.* 2014;44:234–239.
48. Gurtu V, Kain SR, Zhang G. Fluorometric and colorimetric detection of caspase activity associated with apoptosis. *Anal Biochem.* 1997;251(1):98–102.
49. Nylander E, Grönbladh A, Zelleröth S, et al. Growth hormone is protective against acute methadone-induced toxicity by modulating the NMDA receptor complex. *Neurosci.* 2016;339:538–547.